

CRL-VLA: Continual Vision–Language–Action Learning

Qixin Zeng¹ **Shuo Zhang**² **Hongyin Zhang**² **Renjie Wang**² **Han Zhao**² **Libang Zhao**² **Runze Li**²
Donglin Wang^{2†} **Chao Huang**^{1†}

Abstract

Lifelong learning is critical for embodied agents in open-world environments, where reinforcement learning fine-tuning has emerged as an important paradigm to enable Vision–Language–Action (VLA) models to master dexterous manipulation through environmental interaction. Thus, Continual Reinforcement Learning (CRL) is a promising pathway for deploying VLA models in lifelong robotic scenarios, yet balancing stability (retaining old skills) and plasticity (learning new ones) remains a formidable challenge for existing methods. We introduce CRL-VLA, a framework for continual post-training of VLA models with rigorous theoretical bounds. We derive a unified performance bound linking the stability–plasticity trade-off to goal-conditioned advantage magnitude, scaled by policy divergence. CRL-VLA resolves this dilemma via asymmetric regulation: constraining advantage magnitudes on prior tasks while enabling controlled growth on new tasks. This is realized through a simple but effective dual-critic architecture with novel Goal-Conditioned Value Formulation (GCVF), where a frozen critic anchors semantic consistency and a trainable estimator drives adaptation. Experiments on the LIBERO benchmark demonstrate that CRL-VLA effectively harmonizes these conflicting objectives, outperforming baselines in both anti-forgetting and forward adaptation.

1. Introduction

Reinforcement Learning (RL) post-training has become a central paradigm for aligning Vision–Language–Action (VLA) models with complex embodied reasoning and robotic manipulation tasks (Black et al., 2024; Kim et al.,

^{*}Equal contribution ¹University of Southampton, UK
²Westlake University, China. Correspondence to: Donglin Wang <wangdonglin@westlake.edu.cn>, Chao Huang <Chao.Huang@soton.ac.uk>.

2025). By optimizing policies through interaction, RL post-training enables adaptive, goal-directed behaviors beyond what supervised learning can provide. Sustaining such adaptability requires lifelong learning across non-stationary task streams. However, in large-scale settings, Continual Reinforcement Learning (CRL) aims to equip agents with the ability to acquire new skills over time without catastrophic forgetting (Sutton, 2019). This problem fundamentally requires balancing scalability, stability, and plasticity under non-stationary task distributions (Pan et al., 2025). Despite its importance, CRL for VLA models remains underexplored, particularly in robotic manipulation scenarios involving multi-modal observations and long-horizon dynamics (Xu & Zhu, 2018; Pan et al., 2025).

Most existing CRL methods enforce stability via parameter- or function-space regularization, but they face severe limitations when applied to modern VLA architectures. Experience replay (Rolnick et al., 2019; Abbes et al., 2025) reuses outdated transitions whose gradients often conflict with those of new tasks, inducing off-policy errors that destabilize continual learning. Second-order regularization methods (Kutalev & Lapina, 2021) are computationally prohibitive due to the scale and dimensionality of multi-modal Transformers (Kim et al., 2025; Li et al., 2024). Recent approaches favor lightweight constraints such as KL regularization (Shenfeld et al., 2025), but such transition-level constraints enforce only short-horizon behavioral similarity and fail to preserve long-term task performance (Korbak et al., 2022). Backbone-freezing strategies (Hancock et al., 2025) hinge on the fragile assumption that pretrained multi-modal representations remain aligned with language goals; under task shifts, value learning drifts without explicit language conditioning, degrading adaptation and collapsing plasticity (Jiang et al., 2025b; Guo et al., 2025).

In this work, we show that forgetting in continual VLA learning is fundamentally driven by the goal-conditioned advantage magnitude, which directly links policy divergence to performance degradation on prior tasks. This perspective reframes the stability–plasticity dilemma as an asymmetric regulation problem: *suppressing advantage magnitudes on previous tasks to ensure stability, while permitting controlled growth on new tasks to enable plasticity*.

Based on this insight, we propose **CRL-VLA**, a continual learning framework that disentangles stable value semantics from adaptive policy learning via a novel **Goal-Conditioned Value Formulation (GCVF)**. Our method employs a dual-critic architecture in which a frozen critic anchors long-horizon, language-conditioned value semantics, while a trainable critic estimator drives adaptation. Stability is further enforced by combining trajectory-level value consistency with transition-level KL regularization, while Monte Carlo (MC) estimation and standard RL objectives support efficient learning on new tasks without catastrophic forgetting. Our contributions are summarized as follows:

- We propose **CRL-VLA**, a principled continual post-training framework for VLA models that identifies the goal-conditioned advantage magnitude as the key quantity governing the stability–plasticity trade-off.
- CRL-VLA operationalizes this insight via a dual-critic architecture with a novel goal-conditioned value formulation, enabling asymmetric regulation that preserves prior skills while efficiently adapting to new tasks.
- Extensive experiments show that CRL-VLA consistently outperforms strong baselines on continual VLA benchmarks, achieving superior knowledge transfer and resistance to catastrophic forgetting.

2. Related work

2.1. Reinforcement Learning for VLA Models

VLA models have gained interest as unified robotic manipulation policies, with recent work exploring online RL to address SFT limitations and improve generalization and long-horizon reasoning. SimpleVLA-RL (Li et al., 2025) builds upon OpenVLA-OFT and GRPO, showing that online RL substantially improves long-horizon planning under demonstration scarcity. RIPT-VLA (Tan et al., 2025) applies the REINFORCE leave-one-out estimator to QueST and OpenVLA-OFT architectures. ARFM (Zhang et al., 2025a) enhances VLA action models via adaptive offline RL, balancing signal and variance to improve generalization and robustness. RLinf-VLA (Zang et al., 2025) implements a novel hybrid fine-grained pipeline allocation mode scaling up VLA model training with diverse RL algorithms and benchmarks. Recent work introduces IRL-VLA, a closed-loop RL framework for VLA autonomous driving that achieved award-winning performance in benchmarks (Jiang et al., 2025a). In contrast, our work aims to investigate the knowledge transfer of VLA models and their ability to learn new tasks stably and continuously.

2.2. Continual Reinforcement Learning

Continual reinforcement learning generally falls into three paradigms. Regularization-based methods constrain updates to important parameters using Fisher information (Aich, 2021) or path integrals (Zenke et al., 2017), or enforce behavioral consistency via KL divergence (Shenfeld et al., 2025). Replay-based strategies (Rolnick et al., 2019) mitigate forgetting by interleaving past experience, though recent benchmarks (Wolczyk et al., 2021) highlight their scalability limits in high-dimensional robotics. Architecture-based approaches (Xu & Zhu, 2018) prevent interference by expanding network capacity, a strategy often impractical for large-scale pretrained models. While limited works explore value preservation via distillation (Schwarz et al., 2018; Rusu et al., 2016), they typically neglect the value drift inherent in non-stationary, language-conditioned tasks. Unlike these approaches, our work focuses on the continuous learning process of VLA models for general visual language manipulation tasks.

2.3. Continual learning in VLA model

To date, there are no studies on continual learning specifically for VLA models, but similar research methods exist. Recent work (Yadav et al., 2025) improves policy stability under task variations, providing useful insights for subsequent lifelong learning approaches, although it is evaluated in a non-continual setting. Recently, several works have extended these paradigms to the VLA domain. VLM2VLA (Hancock et al., 2025) treats actions as a special language tokens and employs LoRA to align pre-trained VLMs with low-level robot control. Stellar-VLA (Wu et al., 2025) introduces a skill-centric knowledge space to evolve task representations continually across diverse robot manipulation scenarios. DMPEL (Lei et al., 2025) proposes a dynamic mixture of progressive parameter-efficient experts to achieve lifelong learning without high storage overhead. ChatVLA (Zhou et al., 2025) addresses spurious forgetting by decoupling multi-modal understanding from high-frequency action execution. Unlike these work, we aim to investigate a continuous post-training framework for VLA models and explicitly model the stability-plasticity trade-off between new and old tasks.

3. Preliminaries

We study continual post-training of VLA policies in a goal-conditioned reinforcement learning setting. Each task is formulated as a goal-conditioned MDP $\mathcal{M} = \langle \mathcal{S}, \mathcal{A}, \mathcal{G}, P, r, \gamma \rangle$, where $s \in \mathcal{S}$ is the state, $g \in \mathcal{G}$ is a language instruction, and $a \in \mathcal{A}$ is a robotic control command. For a given policy π and goal g , we define the state-value function as $V^\pi(s, g) = \mathbb{E}_{\tau \sim \pi, g} [\sum_{t=0}^{\infty} \gamma^t r(s_t, a_t, g) | s_0 = s]$, which represents the expected cumulative return start-

ing from state s . The action-value function is defined as $Q^\pi(s, a, g) = \mathbb{E}[\sum_{t=0}^{\infty} \gamma^t r(s_t, a_t, g) | s_0 = s, a_0 = a]$. The advantage function $A^\pi(s, a, g) = Q^\pi(s, a, g) - V^\pi(s, g)$ measures how much better an action is compared to the average action at that state.

The state occupancy measure $d_g^\pi(s) = (1 - \gamma)\mathbb{E}[\sum_{t=0}^{\infty} \gamma^t \mathbf{1}(s_t = s)]$ describes the distribution of states visited by policy π when executing goal g . Different policies induce different state visitation distributions, which is fundamental to understanding how policy updates affect task performance. The goal-conditioned policy is $\pi(a | s, g)$, with expected return for goal g given by $J_g(\pi) = \mathbb{E}_{\tau \sim \pi, g} \left[\sum_{t=0}^{\infty} \gamma^t r(s_t, a_t, g) \right]$. Performance on old tasks under distribution $p_{\text{old}}(g)$ is $J_{\text{old}}(\pi) = \mathbb{E}_{g \sim p_{\text{old}}} [J_g(\pi)]$. New policy's performance π' on new tasks under distribution $p_{\text{new}}(g)$ is $J_{\text{new}}(\pi') = \mathbb{E}_{g \sim p_{\text{new}}} [J_g(\pi')]$.

A pretrained VLA policy π_{θ_0} is adapted sequentially to a task stream $\mathcal{T} = \{\mathcal{T}_1, \dots, \mathcal{T}_K\}$. At stage k , the agent interacts only with \mathcal{T}_k and updates to π_k^θ via on-policy RL, without access to interaction data, rewards, or gradients from previous tasks $\{\mathcal{T}_i\}_{i < k}$. For a trajectory $\tau = (s_0, a_0, \dots, s_T)$ with goal g , the MC return at time t is $G_t = \sum_{k=t}^T \gamma^{k-t} r(s_k, a_k, g)$, which provides an unbiased estimate of $V^\pi(s_t, g)$ for critic training. We evaluate using a transfer matrix $\mathbf{R} \in \mathbb{R}^{K \times K}$, where $R_{k,i}$ is the success rate on task \mathcal{T}_i after training through stage k . The objective is to learn a sequence of policies that jointly satisfy three criteria: Plasticity through high performance on the current task, Stability through preserved performance on prior tasks, and Scalability through efficient learning without large buffers or capacity expansion.

4. Methodology

In this section, we first characterize the stability–plasticity dilemma in continual VLA through the advantage magnitude and policy divergence, and then demonstrate that M_{old} and M_{new} can be controlled in a decoupled manner. Furthermore, we introduce a dual goal-conditioned critic for continual VLA and then present the corresponding objectives, regularization, and training recipe.

4.1. The Stability–Plasticity Dilemma in Continual VLA

At stage k of continual VLA post-training, we update the policy π^k with two coupled criteria. **Plasticity** means the maximization of new-goal return $J_{g_k}(\pi^k; \mathcal{T}_k)$, while **stability** is the bounded degradation of old-goal return under the

same update. Therefore, we solve

$$\max_{\pi^k} J_{g_k}(\pi^k; \mathcal{T}_k) \quad (1)$$

$$\text{s.t. } J_{g_{k-1}}(\pi^k; \mathcal{T}_{k-1}) \geq J_{g_{k-1}}(\pi^{k-1}; \mathcal{T}_{k-1}) - \delta. \quad (2)$$

Here, each task T_k in the sequence $T = \{T_1, \dots, T_K\}$ specifies a goal g_k , and the agent iteratively updates its policy π_k^θ via reinforcement learning under a bound δ on degradation over prior tasks. However, directly measuring the return impact of policy divergence during task transition is intractable. We therefore seek a bridge that links policy divergence to return change. In continual reinforcement learning for VLA model, we introduce the advantage magnitude M_g .

Definition 4.1. For any policy π^κ and goal g , we define the *Advantage Magnitude*, denoted as $M_g(\pi^\kappa)$, as the maximum absolute advantage of the anchored policy π (typically set as the previous policy π^{old}) evaluated over the state-action pairs visited by π^κ :

$$M_g(\pi^\kappa) \triangleq \sup_{(s, a) \in \text{supp}(d_g^{\pi^\kappa})} |A^\pi(s, a)|. \quad (3)$$

Here, $M_g(\pi^\kappa)$ close to 0 indicates that the policy aligns closely with the anchored policy on the evaluated distribution. Based on Definition 4.1, we evaluate a post-update policy π^{new} under the old-goal distribution p_{old} of old task and the new-goal distribution p_{new} of new task. We then define two metrics to quantify the stability–plasticity trade-off. The **Stability Metric** M_{old} measures the maximum advantage of the old policy over its own state distribution, capturing performance retention on old tasks. The **Plasticity Metric** M_{new} measures the maximum advantage achievable on new tasks under the new policy:

$$\begin{aligned} M_{\text{old}} &\triangleq \mathbb{E}_{g_{\text{old}} \sim p_{\text{old}}} [M_{g_{\text{old}}}(\pi^{\text{new}})], \\ M_{\text{new}} &\triangleq \mathbb{E}_{g_{\text{new}} \sim p_{\text{new}}} [M_{g_{\text{new}}}(\pi^{\text{new}})]. \end{aligned} \quad (4)$$

A Unified Perspective on Stability and Plasticity. Theorem 4.1 establishes a unified perspective on the stability–plasticity trade-off in goal-conditioned continual learning. Both performance degradation on old tasks and performance improvement on new tasks are governed by the coupling mechanism of advantage magnitude and policy divergence measured by KL divergence.

This unified bound suggests that controlling continual learning reduces to balancing these two coupled quantities on old and new tasks. We next discuss how M_{old} and D_{old} govern stability, and how M_{new} and D_{new} govern plasticity. **1) Old-task stability.** M_{old} characterizes the sensitivity of old-task returns to policy changes, while D_{old} quantifies the policy change magnitude under the old-task state distribution; the $(1 - \gamma)^{-2}$ scaling factor amplifies this coupling in long-horizon settings. **2) New-task plasticity.** M_{new}

reflects the policy improvement potential, while D_{new} measures the policy modification degree under the new-task state distribution. Plasticity requires large policy modifications (D_{new}) combined with learning potential (M_{new}); conversely, constraining D_{new} to preserve old-task performance limits achievable improvement on new tasks.

However, the coupling challenge remains stability and plasticity are fundamentally coupled through policy divergence under different state distributions. Common continual learning methods impose global constraints on policy updates via trust-region or KL penalties, restricting policy changes across all state space regions (Kessler et al., 2022). Reducing D_{old} to tighten the old-task stability bound also reduces D_{new} , thereby limiting plasticity on new tasks. Therefore, an effective trade-off requires minimizing M_{old} while constraining policy divergence under both old-task and new-task distributions with controllable M_{new} .

Theoretical Result

Theorem 4.1 (Unified Stability-Plasticity Bounds). *Let π^{new} and π^{old} be the new and old policies. $J_{\text{old}}(\pi)$ and $J_{\text{new}}(\pi)$ denote the expected returns of policy π on the old and new tasks, respectively. The policy divergence parameters D_{old} and D_{new} directly use the expected KL divergence:*

$$D_{\text{old}} \triangleq \sqrt{2 \mathbb{E}_{s \sim d_{\text{old}}^{\pi^{\text{old}}}} [D_{\text{KL}}(\pi^{\text{new}}(\cdot|s) \| \pi^{\text{old}}(\cdot|s))]},$$

$$D_{\text{new}} \triangleq \sqrt{2 \mathbb{E}_{s \sim d_{\text{new}}^{\pi^{\text{new}}}} [D_{\text{KL}}(\pi^{\text{new}}(\cdot|s) \| \pi^{\text{old}}(\cdot|s))]}.$$

The performance variations are bounded by:

$$|J_{\text{old}}(\pi^{\text{new}}) - J_{\text{old}}(\pi^{\text{old}})| \leq \frac{2\gamma}{(1-\gamma)^2} \cdot M_{\text{old}} \cdot D_{\text{old}},$$

$$J_{\text{new}}(\pi^{\text{new}}) - J_{\text{new}}(\pi^{\text{old}}) \leq \frac{1}{1-\gamma} \cdot M_{\text{new}} \cdot D_{\text{new}}.$$

Proof. Using Performance Difference Lemma (Kakade & Langford, 2002) and discounted occupancy bounds (Achiam et al., 2017), we derive performance difference bounds between old and new policies under goal-conditioned task transitions. Full derivations are in Appendix A.2. \square

Remark 4.1. An effective stability-plasticity trade-off requires minimizing M_{old} while constraining D_{old} and D_{new} with controllable M_{new} .

4.2. Decouple control for Stability and Plasticity Metrics

The central question becomes: can we control stability metrics M_{old} and plasticity metrics M_{new} separately? The answer depends on understanding the fundamental differences

between these two quantities. Corollaries 4.1-4.2 reveal these two metrics are bounded by independent factors with concrete derivations in Appendix A.4. M_{old} is constrained by critic approximation error ε_V on \mathcal{D}_{old} , while M_{new} is limited by environment return range $[G_{\min}, G_{\max}]$. Since ε_V operates on replay data and environment return range is task-intrinsic, a single constraint cannot regulate both. This necessitates dual mechanisms: minimizing ε_V via constrained updates on \mathcal{D}_{old} controls M_{old} , while MC-based estimation on new tasks exploits natural boundedness to control M_{new} . The orthogonality of these mechanisms enables simultaneous stability and plasticity without trade-offs: we control M_{old} by minimizing ε_V on old task data, while M_{new} remains naturally bounded by the environment’s return range during new task learning.

Corollary [V-only Path Bound]

Corollary 4.1 (Controllability of Stability). *Let V_{θ} denote the parameterized approximation and V_{old} the true anchor value. Under bounded rewards $|r(s, a, g_{\text{old}})| \leq R_{\max}$ and error $\varepsilon_V \triangleq \sup_{s, g_{\text{old}}} |V_{\theta} - V_{\text{old}}|$, the advantage magnitude on old tasks satisfies: $M_{\text{old}} \leq R_{\max} + (1+\gamma)\varepsilon_V + (1+\gamma)\|V_{\text{old}}\|_{\infty}$.*

Remark 4.2. The bound reveals that M_{old} can be directly controlled by constraining the value approximation error ε_V on old tasks.

Corollary [V-only Path Bound]

Corollary 4.2 (Natural Boundedness of Plasticity). *Let G_t^g be the ground-truth MC return for goal g , with $G_t^g \in [G_{\min}, G_{\max}]$, at any time t . Then, for the V-only advantage estimator $\hat{A}_{g_{\text{new}}}(s, a)$, the advantage magnitude M_{new} satisfies: $M_{\text{new}} \leq 2(1+\gamma) \max\{|G_{\min}|, |G_{\max}|\}$.*

Remark 4.3. The bound reveals that M_{new} can be directly controlled by bounding by reward of MC estimator.

4.3. Dual Goal-Conditioned Critic for continual VLA

Given that D_{old} and D_{new} in Theorem 4.1 are realized via KL divergence, we develop value functions that make advantage magnitudes M_g controllable, serving as a surrogate for direct advantage-based optimization. Furthermore, we enhance language-following capacity by conditioning the value network directly on language embeddings. Inspired by Corollaries 4.1 and 4.2, we propose a simple yet effective dual-critic framework.

Infeasibility of Direct Advantage Optimization in VLA

Obtaining accurate advantage estimates in VLA settings

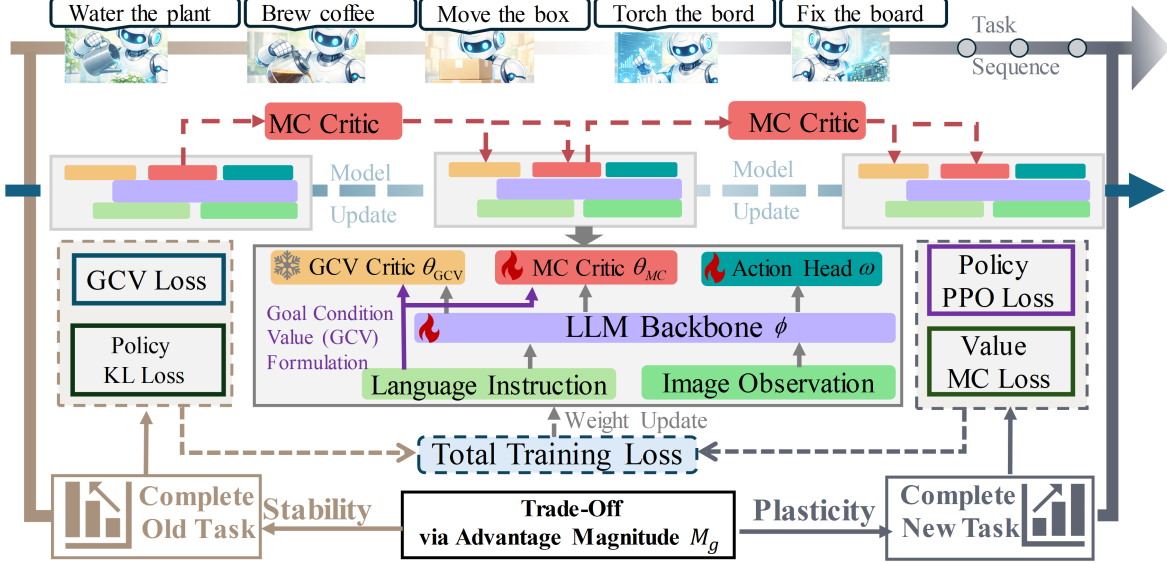


Figure 1. The proposed CRL-VLA method. CRL-VLA is a continuous learning framework for VLA models that treats the goal-conditioned advantage magnitude as a key factor determining the trade-off between stability and plasticity. CRL-VLA achieves this insight through a dual critic architecture and a PPO loss with several regularization terms, enabling asymmetric tuning that efficiently adapts to new tasks while preserving prior knowledge.

requires expensive multi-step rollouts and bootstrapping, which is hard to scale (Chen et al., 2023). Concretely, for large VLA policies deployed on real robots or high-fidelity simulators, each additional rollout entails a full forward pass of a vision–language backbone plus action decoding, making per-update advantage estimation extremely costly (Wen et al., 2024). Therefore, in continual VLA settings, MC estimation is preferred the TD bootstrapping due to prohibitive computational costs in scaling models and the bias inherent in value estimation.

Indirect Control via Value Functions Corollaries 4.1 and 4.2 demonstrate that the theoretical upper bounds on the performance gap can be expressed through value functions. Guided by this insight, we control M_g indirectly via value estimation rather than imposing direct constraints on the advantage network. While value estimation can be realized through either state-value functions or action-value functions, we focus on the state-value function $V(s, g)$ in the main text for conciseness; the extension to action-value functions is detailed in Appendix B.2. Specifically, for a given VLA policy π and language goal g , we approximate the advantage function $\hat{A}_g(s, a)$ as: $\hat{A}_g(s, a) = r(s, a, g) + \gamma V_\pi(s', g) - V_\pi(s, g)$, where $s \sim d_g^\pi$ is a state sampled from the goal-conditioned state distribution, $s' \sim \mathcal{P}(\cdot|s, a)$ is the successor state, $V_\pi(\cdot, g)$ is the state-value function for goal g under policy π , and $\gamma \in (0, 1)$ is the discount factor.

Goal-Conditioned Value Formulation To condition the value function on language goal g , we leverage the shared Vision-Language Model’s embedding as the global state representation. Specifically, we concatenate language embedding with global state representations before the MLP (Figure 1), which outputs the scalar value $V(s, g)$. This joint encoding addresses the poor language-goal following capacity in VLA value heads (Intelligence et al., 2025).

Dual-Critic Architecture for Independent Dimension Management To operationalize indirect control of M_g , we design a dual-critic architecture as follows.

1. **Frozen Goal-Conditioned Value (GCV) Critic θ_{GCV} .** Initialized from the old task’s value network and frozen during new task training, it provides the reference value $V_{\text{old}}(s, g)$ for Corollary 4.1, enabling regularization of value accuracy differences on old data while maintaining predictable bounds via value drift prevention.
2. **Trainable MC critic θ_{MC} .** Updated on new task MC returns to implement Corollary 4.2, allowing natural emergence of M_{new} bounds.

Overall, the shared backbone ϕ serves as a unified feature extractor, while head decoupling enables targeted optimization. Specifically, the frozen GCV critic θ_{GCV} preserves value consistency and constrains value approximation error, guiding the action head ω to favor high-return actions in old task states. While the trainable MC critic θ_{MC} bounds growth while maintaining plasticity for continual learning.

4.4. Regularization and Training Recipe

We instantiate Theorem 4.1 with Corollaries 4.1 and 4.2 through three mechanisms that balance stability and plasticity by controlling M_{old} , M_{new} , D_{new} , and D_{old} . This unified algorithm applies to both state and action value functions, with the latter detailed in Appendix B.2.

First, we control M_{old} through Goal-Conditioned Value (GCV) consistency. At task transition, the converged MC critic is copied to θ_{GCV} and frozen. During new task training, backbone updates ϕ are penalized when $V_{\phi, \theta_{\text{GCV}}}$ deviates from V_{old} . At task transition, we freeze the converged MC critic as θ_{GCV} anchored to reference values $V_{\text{old}}(s, g)$ from \mathcal{B}_{old} to minimize ε_V on the old task distribution, as required by Corollary 4.1. We constrain M_{old} by ensuring the new policy generates trajectory-level action distributions consistent with the old policy when evaluated on sampled states $(s, g) \in \mathcal{B}_{\text{old}}$ from previous tasks. This is achieved through the following loss:

$$\mathcal{L}_{\text{GCV}}^V(\phi) = \beta_V \mathbb{E}_{(s, g) \sim \mathcal{B}_{\text{old}}} \left[\|V_{\phi, \theta_{\text{GCV}}}(s, g) - V_{\text{old}}(s, g)\|^2 \right]. \quad (5)$$

Second, we realize bounded M_{new} via MC Critic learning. Since the Corollary 4.2 directly shows controllable M_{new} is bounded by MC return $G_t^{g_{\text{new}}}$ during roll-out. Combined with dense reward shaping (Zhang et al., 2025b), this achieves accurate advantage estimation without constraining backbone plasticity. Thus, we train a learnable MC Critic critic θ_{MC} on new task trajectories:

$$\mathcal{L}_{\text{MC}}^V(\theta_{\text{MC}}, \phi) = \mathbb{E}_{(s, g) \sim \mathcal{B}_{\text{new}}} \left[\|V_{\phi, \theta_{\text{MC}}}(s, g) - G_t^{g_{\text{new}}}\|^2 \right]. \quad (6)$$

Our third mechanism constrains policy divergence D_{new} and D_{old} to control distribution shift. PPO’s trust region constraint (Eq. 15, Appendix B.1) limits the π updates in the distribution of new task, thereby bounding D_{new} drift. To maintain D_{old} (Theorem 4.1), we propose

$$\mathcal{L}_{\text{KL}}(\phi, \omega) = \mathbb{E}_{(s, g) \sim \mathcal{B}_{\text{old}}} [D_{\text{KL}}(\pi_{\text{old}}(\cdot | s, g) \| \pi(\cdot | s, g))], \quad (7)$$

where π_{old} is the old policy that generated \mathcal{B}_{old} . The total training loss integrates these constraints:

$$\mathcal{L}_{\text{total}} = \mathcal{L}_{\text{PPO}} + \alpha \mathcal{L}_{\text{KL}} + \beta_V \mathcal{L}_{\text{GCV}}^V + \eta \mathcal{L}_{\text{MC}}^V. \quad (8)$$

This Lagrangian relaxation of Eq. (1) instantiates Theorem 4.1’s dual constraints, with concrete derivations in appendix A.5. \mathcal{L}_{PPO} and \mathcal{L}_{KL} bound D_{new} and D_{old} (policy divergence), while $\mathcal{L}_{\text{GCV}}^V$ and $\mathcal{L}_{\text{MC}}^V$ bound M_{old} and enable M_{new} exploitation (value accuracy and plasticity). Hyperparameters α, β_V, η act as Lagrange multipliers controlling the stability-plasticity tradeoff. Overall, the CRL-VLA pipeline has been summarized in Alg. 1.

Algorithm 1 CRL-VLA: VLA Policy Continuous Learning

Require: Pretrained VLA policy π_{θ_0} , tasks $\{\mathcal{T}_k\}_{k=1}^K$.

```

1: for  $k = 1$  to  $K$ :
2:   if  $k = 1$ :
3:     Train  $\pi_{\theta_1}$  on  $\mathcal{T}_1$  using standard RL
4:     Freeze  $\pi_{\theta_1}$  and its value function as  $\pi^{\text{old}}$ ,  $V_{\text{old}}$ 
5:     Store replay buffer  $\mathcal{B}_{\text{old}}$ 
6:   else:
7:     for each training iteration:
8:       Collect new task trajectories  $\tau \sim \pi_{\theta}$  on  $\mathcal{T}_k$ 
9:       Sample batch  $\mathcal{B}_{\text{new}} \sim \tau$ ,  $\mathcal{B}_{\text{old}} \sim \mathcal{D}_{\text{old}}$ 
10:      Compute losses  $\mathcal{L}_{\text{total}}$  by Eq. 13
11:      Update  $\theta$  via gradient descent on  $\mathcal{L}_{\text{total}}$ 
12:   Continually adapted VLA policies  $\{\pi_{\theta_k}\}_{k=1}^K$ 

```

5. Experiments

In this section, we explore how the CRL-VLA effectively achieves a balance between stability and plasticity, thereby enhancing the robot’s continuous learning ability for visual language manipulation tasks. To this end, our experiments aim to investigate the following questions: **1)** Compared to baseline algorithms, does CRL-VLA exhibit better adaptability and resistance to forgetting when performing a single long-horizon task? **2)** Compared to baseline algorithms, does CRL-VLA exhibit superior cross-task knowledge sharing and transfer performance when performing multiple long-horizon tasks? **3)** How important are the core components of the proposed method to the overall learning performance of the CRL-VLA framework?

5.1. Setup

To comprehensively evaluate the performance of the proposed CRL-VLA, we constructed a set of VLA model continuous learning task settings based on the LIBERO (Liu et al., 2023) benchmark. Specifically, we constructed benchmark subsets by randomly sampling tasks from the LIBERO shared task pool. These subsets contain tasks randomly sampled from the original dataset to cover different task scales. Each benchmark contains multiple sets of tasks defined by language instructions. See Appendix C for specific task settings. Furthermore, we used the same OpenVLA-oft model and PPO post-training configuration for all algorithms (Tan et al., 2025; Kim et al., 2025). To systematically answer the first and second questions, two types of experimental settings were primarily considered: **1)** Single-task learning scenarios: used to evaluate the adaptability of each algorithm to a specific task; **2)** Multi-task learning scenarios: used to evaluate the cross-task knowledge sharing and continuous learning performance of each algorithm.

Baselines. To thoroughly compare the superiority of the CRL-VLA, we consider several classic CL algorithms. **1)** Sequence Learning (SL) (Liu et al., 2023): This is the most direct CL algorithm. The VLA model is only fine-tuned for new tasks, without any specific mechanism to prevent forgetting. **2)** Learning Without Forgetting (LWF) (Li & Hoiem, 2017): This baseline algorithm retrains the VLA model using only new task data while preserving the model’s original functionality. **3)** Experience Replay (ER) (Lopez-Paz & Ranzato, 2017): This baseline algorithm stores sample data from past tasks and converts them into gradient constraints, achieving gradient contextual memory. **4)** Multi-Task Learning (MTL) (Liu et al., 2023): This baseline algorithm learns from both new and old tasks simultaneously. Our method includes two versions: one using V-based goal-conditioned value (**CRL-VLA (V)**) and the other using Q-based goal-conditioned value (**CRL-VLA (Q)**).

Evaluation Metrics. To systematically evaluate the performance of each algorithm, we adopted three standard metrics widely used in CRL benchmarks (Wolczyk et al., 2021): **1) Final Performance; 2) Stability and Forgetting; 3) Plasticity and Forward Transfer.** Specifically, the **Final Performance** metric represents the overall task performance of the VLA model after continuous training, and is measured by the Final Average Return (**FAR**): $\text{FAR} := \frac{1}{T} \sum_{i=1}^T R_{T,i}$. This metric reflects the average success rate of the VLA model across all tasks in the post-training phase. **Stability and Forgetting** metrics are evaluated using Backward Transfer (**BWT**), which measures how learning a new task affects the performance of previously learned tasks: $\text{BWT} := \frac{1}{T-1} \sum_{i=1}^{T-1} (R_{T,i} - R_{i,i})$. A negative BWT indicates a catastrophic forgetting rate in the VLA model. To explicitly quantify forgetting, we further define the Forgetting (**F**) metric for the VLA model: $F_i := \max_{k \geq i} R_{k,i} - R_{T,i}$, $F := \frac{1}{T-1} \sum_{i=1}^{T-1} F_i$. This metric measures the degree of degradation from peak performance to final performance for each task. **Plasticity and Forward Transfer** metrics are evaluated using Forward Transfer (**FT**), which reflects the extent to which prior knowledge facilitates the learning of new tasks. Let b_i represent the baseline success rate of task \mathcal{T}_i before learning previous tasks. We define: $\text{FT} := \frac{1}{T-1} \sum_{i=2}^T (R_{i-1,i} - b_i)$, where a positive value indicates a beneficial forward transition in the VLA model.

5.2. Main Results

Single-task learning scenario. Tab. 1 compares the continuous learning performance of various algorithms in single-task learning scenarios. The results show that, compared to the baselines, the CRL-VLA (Q) has the highest FAR metric value (0.98), the second highest BWT metric value (−0.02), and the lowest F metric value (0.03). Except

Table 1. Performance comparison on the single-task learning scenario. Specific task settings in Appendix C.1. ↑ denotes higher is better, ↓ denotes lower is better. Best results are **bold**, and second best are underlined.

Method	FAR (↑)	BWT (↑)	FT (↑)	F (↓)
SL (Liu et al., 2023)	0.00	-0.62	-0.50	0.62
MTL (Liu et al., 2023)	<u>0.96</u>	0.11	-0.06	<u>0.06</u>
ER (Lopez-Paz & Ranzato, 2017)	0.60	-0.51	-0.06	0.53
LWF (Li & Hoiem, 2017)	0.67	-0.50	-0.06	0.50
CRL-VLA (V)	0.67	-0.49	-0.06	0.50
CRL-VLA (Q)	0.98	<u>-0.02</u>	-0.06	0.03

for the SL baseline algorithm (−0.5), the other methods exhibit similarly high FT metric values (−0.06). Therefore, our method has better overall task success rate and resistance to forgetting old tasks, thus enabling more continuous and stable learning of new tasks. This also confirms that our method allows the VLA model to better balance task stability and plasticity during continuous learning.

Table 2. Performance comparison on the multi-task learning scenario. Specific task settings in Appendix C.2.

Method	FAR (↑)	BWT (↑)	FT (↑)
SL (Liu et al., 2023)	0.62	0.07	0.25
MTL (Liu et al., 2023)	0.49	0.00	0.25
ER (Lopez-Paz & Ranzato, 2017)	0.62	0.05	0.00
LWF (Li & Hoiem, 2017)	0.63	<u>0.10</u>	<u>0.00</u>
CRL-VLA (V)	0.74	0.17	0.00
CRL-VLA (Q)	<u>0.66</u>	-0.03	0.00

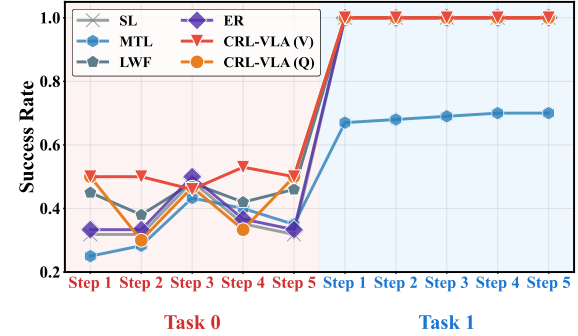


Figure 2. Performance comparison of various algorithms during continual learning. Specific task settings in Appendix C.2.

Multi-task learning scenario. To further examine whether the proposed method CRL-VLA possesses better cross-task knowledge sharing and continuous learning capabilities in multi-task learning scenarios, we conducted a performance comparison experiment (Tab. 2). The experimental results show that, compared to the baseline algorithms, our method CRL-VLA (V) has the highest FAR metric value (0.74) and the highest BWT metric value (0.17). Furthermore, regarding the FT metric values, SL and MTL have the highest values (0.25), while other methods have the

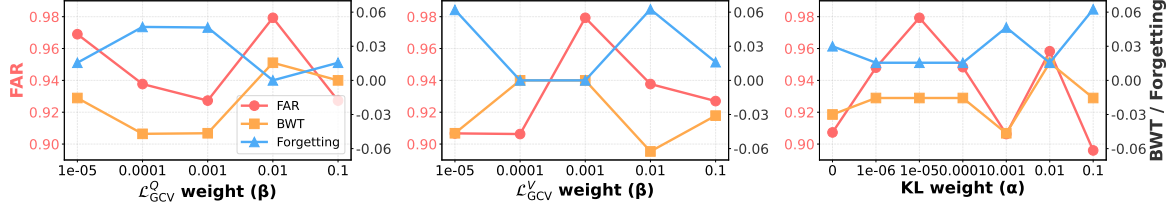


Figure 3. The impact of different values of the loss weights of $\mathcal{L}_{\text{GCV}}^Q$ (left), $\mathcal{L}_{\text{GCV}}^V$ (middle), and policy KL (right) on the continuous learning performance of the VLA model. Specific task settings in Appendix C.4.

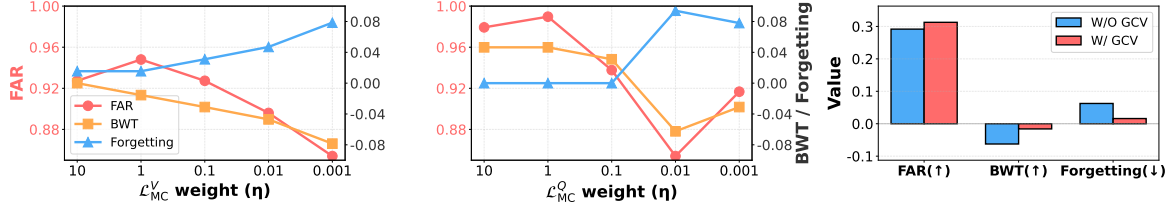


Figure 4. The impact of different values of the loss weights of $\mathcal{L}_{\text{MC}}^V$ (left) and $\mathcal{L}_{\text{MC}}^Q$ (middle) on the continuous learning performance of the VLA model, and an ablation comparison with and without GCV (right). Specific task settings in Appendix C.4.

same value (0.). Therefore, in multi-task learning scenarios, compared to the baseline, our method possesses better cross-task knowledge sharing and anti-forgetting capabilities, thus exhibiting better continuous learning capabilities. Moreover, the experiment result also demonstrates that our method can significantly improve the overall task success rate of the VLA model, and the performance comparison of each algorithm during the continuous learning process in Fig. 2 further confirms this. For more performance comparisons in multi-task learning scenarios, see Appendix Tab. 3.

Furthermore, experimental results (Tab. 1 and Tab. 2) also show that $\mathcal{L}_{\text{GCV}}^Q$ is more effective in single-task learning, while $\mathcal{L}_{\text{GCV}}^V$ performs better in multi-task continuous learning environments. We believe the fundamental reason for this is that in multi-task continuous learning, the state-goal distribution becomes more diverse, and similar states may correspond to multiple effective action implementations in different tasks. $\mathcal{L}_{\text{GCV}}^Q$ constrains value consistency at the action-condition level, implicitly enforcing outdated action semantics sampled from previous tasks, which may conflict with the current learning objective. In contrast, $\mathcal{L}_{\text{GCV}}^V$ operates at the state-goal level and marginalizes actions, thus maintaining robustness to increased action diversity while preserving long-horizon value semantics.

5.3. Ablation Study

We first conduct ablation experiments on the GCV loss weights and policy KL loss weights in the CRL-VLA to evaluate the contribution of the GCV and policy KL components to the continuous learning performance of VLA. The experimental results are shown in Fig. 3. For $\mathcal{L}_{\text{GCV}}^Q$ and $\mathcal{L}_{\text{GCV}}^V$ losses, moderate loss weights (approximately

0.01 and 0.001 respectively) yield better FAR and BWT, as well as lower forgetting, achieving a better post-training stability-plasticity balance for the VLA model. Furthermore, excessively small weights fail to suppress M_{old} , while excessively large weights over-constrain updates and reduce forward adaptation. On the other hand, moderate policy KL term weights α perform best (approximately 0.01). An excessively strong KL term narrows the feasible update region and indirectly inhibits the effective use of M_{new} , while an excessively weak KL term leads to policy drift, potentially increasing the actual M_{old} even with critic anchoring.

We further conduct ablation experiments on the value loss MC weights (Fig. 4, left and middle). The results show that the VLA model exhibits the best sustained learning performance when the weights of $\mathcal{L}_{\text{MC}}^V$ and $\mathcal{L}_{\text{MC}}^Q$ are approximately 1. When the value loss weight is too small, the judge error increases, leading to a larger actual advantage and consequently worsening the BWT and forgetting effects; conversely, the optimization process tends to be conservative, potentially reducing the final task performance. This trend confirms that the quality of the critic estimation is a direct means of adjusting M_g , which directly affects the sustained learning performance of the VLA model. Furthermore, experiments comparing the effects of GCV ablation (Fig. 4, right) demonstrate that directly allowing the critic to perceive the language goal brings better success rates, resistance to forgetting, and plasticity to the VLA model.

6. Conclusion and Future Work

In this work, we study continual learning for VLA models and identify the goal-conditioned advantage magnitude as the key factor governing the stability–plasticity trade-off.

Building on this theoretical insight, we propose CRL-VLA, an asymmetric regularization framework realized through a dual-critic architecture with a novel goal-conditioned value formulation. Empirical results demonstrate that CRL-VLA effectively mitigates catastrophic forgetting while maintaining strong forward transfer, outperforming existing baselines. An important direction is extending CRL-VLA to more diverse and unstructured task streams, including partial observability and non-stationary language goals.

References

Abbes, I., Subbaraj, G., Riemer, M., Islah, N., Therien, B., Tabaru, T., Kingetsu, H., Chandar, S., and Rish, I. Revisiting replay and gradient alignment for continual pre-training of large language models. *ArXiv*, abs/2508.01908, 2025. doi: 10.48550/arxiv.2508.01908.

Achiam, J., Held, D., Tamar, A., and Abbeel, P. Constrained policy optimization. In *International conference on machine learning*, pp. 22–31. PMLR, 2017.

Aich, A. Elastic weight consolidation (EWC): nuts and bolts. *CoRR*, abs/2105.04093, 2021. URL <https://arxiv.org/abs/2105.04093>.

Black, K., Brown, T., et al. Pi-0.6: A generalist policy for robotic manipulation. *arXiv preprint arXiv:2410.24192*, 2024.

Chen, Y., Zhang, F., and Liu, Z. Adaptive bias-variance trade-off in advantage estimator for actor-critic algorithms. *Neural networks : the official journal of the International Neural Network Society*, 169:764–777, 2023. doi: 10.1016/j.neunet.2023.10.023.

Guo, Y., Zhang, J., Chen, X., Ji, X., Wang, Y.-J., Hu, Y., and Chen, J. Improving vision-language-action model with online reinforcement learning. *arXiv preprint arXiv:2501.16664*, 2025.

Hancock, A. J., Wu, X., Zha, L., Russakovsky, O., and Majumdar, A. Actions as language: Fine-tuning vlm into vlas without catastrophic forgetting. *arXiv preprint arXiv:2509.22195*, 2025.

Intelligence, P., Black, K., Brown, N., Darpinian, J., Dhabalia, K., Driess, D., Esmail, A., Equi, M., Finn, C., Fusai, N., Galliker, M. Y., Ghosh, D., Groom, L., Hausman, K., Ichter, B., Jakubczak, S., Jones, T., Ke, L., LeBlanc, D., Levine, S., Li-Bell, A., Mothukuri, M., Nair, S., Pertsch, K., Ren, A. Z., Shi, L. X., Smith, L., Springenberg, J. T., Stachowicz, K., Tanner, J., Vuong, Q., Walke, H., Walling, A., Wang, H., Yu, L., and Zhilinsky, U. $\pi_{0.5}$: a vision-language-action model with open-world generalization, 2025. URL <https://arxiv.org/abs/2504.16054>.

Jiang, A., Gao, Y., Wang, Y., Sun, Z., Wang, S., Heng, Y., Sun, H., Tang, S., Zhu, L., Chai, J., et al. Irl-vla: Training an vision-language-action policy via reward world model. *arXiv preprint arXiv:2508.06571*, 2025a.

Jiang, K., Huang, S., Chen, X., Shao, J., Zhang, H., and Li, X. Multimodal continual learning with mllms from multi-scenario perspectives. *arXiv preprint arXiv:2511.18507*, 2025b.

Kakade, S. and Langford, J. Approximately optimal approximate reinforcement learning. In *Proceedings of the nineteenth international conference on machine learning*, pp. 267–274, 2002.

Kessler, S., Parker-Holder, J., Ball, P., Zohren, S., and Roberts, S. J. Same state, different task: Continual reinforcement learning without interference. In *Proceedings of the AAAI Conference on Artificial Intelligence*, volume 36, pp. 7143–7151, 2022.

Kim, M. J., Finn, C., and Liang, P. Fine-tuning vision-language-action models: Optimizing speed and success. *arXiv preprint arXiv:2502.19645*, 2025.

Korbak, T., Perez, E., and Buckley, C. L. RL with KL penalties is better viewed as Bayesian inference. In *Proceedings of the 25th International Conference on Artificial Intelligence and Statistics (AISTATS)*, volume 151 of *Proceedings of Machine Learning Research*, pp. 1083–1091. PMLR, 2022. URL <https://proceedings.mlr.press/v151/korbak22a.html>.

Kutalev, A. and Lapina, A. Stabilizing elastic weight consolidation method in practical ml tasks and using weight importances for neural network pruning. *arXiv preprint arXiv:2109.10021*, 2021.

Lei, Y., Mao, S., Zhou, S., Zhang, H., Li, X., and Luo, P. Dynamic mixture of progressive parameter-efficient expert library for lifelong robot learning. *arXiv preprint arXiv:2506.05985*, 2025.

Li, H., Zuo, Y., Yu, J., Zhang, Y., Yang, Z., Zhang, K., Zhu, X., Zhang, Y., Chen, T., Cui, G., et al. Simplevla-rl: Scaling vla training via reinforcement learning. *arXiv preprint arXiv:2509.09674*, 2025.

Li, X., Lu, F., Tao, M., and Ye, F. X.-F. Robust first and second-order differentiation for regularized optimal transport. *SIAM J. Sci. Comput.*, 47:630–, 2024. doi: 10.48550/arxiv.2407.02015.

Li, Z. and Hoiem, D. Learning without forgetting. *IEEE transactions on pattern analysis and machine intelligence*, 40(12):2935–2947, 2017.

Liu, B., Zhu, Y., Gao, C., Feng, Y., Liu, Q., Zhu, Y., and Stone, P. Libero: Benchmarking knowledge transfer for lifelong robot learning. *Advances in Neural Information Processing Systems*, 36:44776–44791, 2023.

Lopez-Paz, D. and Ranzato, M. Gradient episodic memory for continual learning. *Advances in neural information processing systems*, 30, 2017.

Pan, C., Yang, X., Li, Y., Wei, W., Li, T., An, B., and Liang, J. A survey of continual reinforcement learning. *arXiv preprint arXiv:2506.21872*, 2025.

Rolnick, D., Ahuja, A., Schwarz, J., Lillicrap, T., and Wayne, G. Experience replay for continual learning. In *Advances in Neural Information Processing Systems (NeurIPS)*, volume 32, 2019.

Rusu, A. A., Colmenarejo, S. G., Gulcehre, C., Desjardins, G., Kirkpatrick, J., Kavukcuoglu, K., Pascanu, R., and Hadsell, R. Policy distillation. In *International Conference on Learning Representations*, 2016.

Schulman, J., Wolski, F., Dhariwal, P., Radford, A., and Klimov, O. Proximal policy optimization algorithms. *arXiv preprint arXiv:1707.06347*, 2017.

Schwarz, J. H., Luketina, J., Czarnecki, W. M., Grabska-Barwinska, A., Hessel, M., Kavukcuoglu, K., Kumaran, D., and Teh, Y. W. Progress & compress: A scalable framework for continual learning. In *International Conference on Machine Learning (ICML)*, pp. 4528–4537, 2018.

Shenfeld, I., Pari, J., and Agrawal, P. Rl’s razor: Why online reinforcement learning forgets less. *arXiv preprint arXiv:2509.04259*, 2025.

Sutton, R. S. The bitter lesson, March 2019. Available at <http://www.incompleteideas.net/>.

Tan, S., Dou, K., Zhao, Y., and Krähenbühl, P. Interactive post-training for vision-language-action models, 2025. URL <https://arxiv.org/abs/2505.17016>.

Wen, J., Zhu, Y., Li, J., Zhu, M., Tang, Z., Wu, K., Xu, Z., Liu, N., Cheng, R., Shen, C., Peng, Y., Feng, F., and Tang, J. Tinyvla: Toward fast, data-efficient vision-language-action models for robotic manipulation. *IEEE Robotics and Automation Letters*, 10:3988–3995, 2024. doi: 10.1109/lra.2025.3544909.

Wolczyk, M., Zajac, M., Pascanu, R., Kucinski, L., and Milos, P. Continual world: A robotic benchmark for continual reinforcement learning. In *Advances in Neural Information Processing Systems*, volume 34, pp. 12398–12411, 2021.

Wu, Y., Wang, G., Yang, Z., Yao, M., Sheil, B., and Wang, H. Continually evolving skill knowledge in vision language action model. *arXiv preprint arXiv:2511.18085*, 2025.

Xu, J. and Zhu, Z. Reinforced continual learning. In *Advances in Neural Information Processing Systems (NeurIPS)*, volume 31, pp. 907–916, 2018. URL <https://proceedings.neurips.cc/paper/2018/hash/3229532386db9d77f8ec75591c28b556-Abstract.html>.

Yadav, Y., Zhou, Z., Wagenmaker, A., Pertsch, K., and Levine, S. Robust finetuning of vision-language-action robot policies via parameter merging. *arXiv preprint arXiv:2512.08333*, 2025.

Zang, H., Wei, M., Xu, S., Wu, Y., Guo, Z., Wang, Y., Lin, H., Shi, L., Xie, Y., Xu, Z., et al. Rlinf-vla: A unified and efficient framework for vla+ rl training. *arXiv preprint arXiv:2510.06710*, 2025.

Zenke, F., Poole, B., and Ganguli, S. Continual learning through synaptic intelligence. In *International Conference on Machine Learning (ICML)*, pp. 3987–3995, 2017.

Zhang, H., Zhang, S., Jin, J., Zeng, Q., Qiao, Y., Lu, H., and Wang, D. Balancing signal and variance: Adaptive offline rl post-training for vla flow models. *arXiv preprint arXiv:2509.04063*, 2025a.

Zhang, H., Zhuang, Z., Zhao, H., Ding, P., Lu, H., and Wang, D. Reinbot: Amplifying robot visual-language manipulation with reinforcement learning. *arXiv preprint arXiv:2505.07395*, 2025b.

Zhou, Z., Zhu, Y., Zhu, M., Wen, J., Liu, N., Xu, Z., Meng, W., Peng, Y., Shen, C., Feng, F., et al. Chatvla: Unified multimodal understanding and robot control with vision-language-action model. In *Proceedings of the 2025 Conference on Empirical Methods in Natural Language Processing*, pp. 5377–5395, 2025.

A. Theoretical Analysis and Proofs

A.1. Preliminaries and Definitions

Definition A.1 (Mixture Occupancy Measures). Given a goal distribution $p(g)$, we define the mixture occupancy measure as:

$$d_p^\pi(s) \triangleq \mathbb{E}_{g \sim p}[d_g^\pi(s)],$$

where $d_g^\pi(s) = (1 - \gamma) \sum_{t=0}^{\infty} \gamma^t \Pr(s_t = s \mid g, \pi)$ is the discounted state visitation distribution.

Definition A.2 (Advantage Magnitude). For any policy π^κ and goal g , we define the *Advantage Magnitude*, denoted as $M_g(\pi^\kappa)$, as the maximum absolute advantage of the anchored policy π (typically set as the previous policy π^{old}) evaluated over the state-action pairs visited by π^κ :

$$M_g(\pi^\kappa) \triangleq \sup_{(s, a) \in \text{supp}(d_g^{\pi^\kappa})} |A^\pi(s, a)|. \quad (9)$$

Based on Definition A.2, we define the aggregate stability and plasticity metrics evaluated on the new policy's distribution:

$$M_{\text{old}} \triangleq \mathbb{E}_{g_{\text{old}} \sim p_{\text{old}}}[M_{g_{\text{old}}}(\pi^{\text{new}})], \quad M_{\text{new}} \triangleq \mathbb{E}_{g_{\text{new}} \sim p_{\text{new}}}[M_{g_{\text{new}}}(\pi^{\text{new}})].$$

A.2. Proof of Theorem 4.1

We employ the Goal-Conditioned Performance Difference Lemma (PDL) (Kakade & Langford, 2002):

Lemma A.1 (Goal-Conditioned PDL). *For any policies $\pi^{\text{new}}, \pi^{\text{old}}$ and goal g , the performance difference satisfies:*

$$J_g(\pi^{\text{new}}) - J_g(\pi^{\text{old}}) = \frac{1}{1 - \gamma} \mathbb{E}_{s \sim d_g^{\pi^{\text{new}}}} \left[\mathbb{E}_{a \sim \pi^{\text{new}}(\cdot \mid s, g)} [A_g^{\pi^{\text{old}}}(s, a)] \right].$$

A.2.1. PROOF OF STABILITY BOUND

We aim to bound the performance degradation on old tasks: $|J_{\text{old}}(\pi^{\text{new}}) - J_{\text{old}}(\pi^{\text{old}})|$. Fix a goal $g \sim p_{\text{old}}$. Let $f_g(s) \triangleq \mathbb{E}_{a \sim \pi^{\text{new}}(\cdot \mid s, g)} [A_g^{\pi^{\text{old}}}(s, a)]$. Using Lemma A.1, we decompose the expectation over $d_g^{\pi^{\text{new}}}$:

$$J_g(\pi^{\text{new}}) - J_g(\pi^{\text{old}}) = \frac{1}{1 - \gamma} \left(\underbrace{\mathbb{E}_{s \sim d_g^{\pi^{\text{old}}}} [f_g(s)]}_{\text{(I) Action Mismatch}} + \underbrace{\sum_s (d_g^{\pi^{\text{new}}}(s) - d_g^{\pi^{\text{old}}}(s)) f_g(s)}_{\text{(II) Occupancy Mismatch}} \right).$$

Bounding the Supremum Term: Note that for any state $s \in \text{supp}(d_g^{\pi^{\text{new}}})$ and action $a \sim \pi^{\text{new}}(\cdot \mid s, g)$, the pair (s, a) falls within the support of the visiting policy. By Definition A.2:

$$|f_g(s)| = |\mathbb{E}_{a \sim \pi^{\text{new}}} [A_g^{\pi^{\text{old}}}(s, a)]| \leq \sup_a |A_g^{\pi^{\text{old}}}(s, a)| \leq M_g(\pi^{\text{new}}).$$

Term (II) Occupancy Mismatch: This term represents the drift in state distribution. Applying Hölder's inequality and the discounted occupancy bound (Achiam et al., 2017):

$$|\text{Term (II)}| \leq \|d_g^{\pi^{\text{new}}} - d_g^{\pi^{\text{old}}}\|_1 \cdot \sup_{s \in \text{supp}(d_g^{\pi^{\text{new}}})} |f_g(s)|.$$

Substituting the bounds:

$$|\text{Term (II)}| \leq \left(\frac{2\gamma}{1 - \gamma} \mathbb{E}_{s \sim d_g^{\pi^{\text{old}}}} [D_{\text{TV}}(\pi^{\text{new}} \parallel \pi^{\text{old}})] \right) \cdot M_g(\pi^{\text{new}}).$$

Applying Pinsker's inequality ($D_{\text{TV}} \leq \sqrt{\frac{1}{2} D_{\text{KL}}}$) and substituting back into the PDL (multiplying by $\frac{1}{1 - \gamma}$):

$$\text{Error}_{\text{occ}} \leq \frac{2\gamma}{(1 - \gamma)^2} M_g(\pi^{\text{new}}) \cdot \mathbb{E}_{s \sim d_g^{\pi^{\text{old}}}} \left[\sqrt{\frac{1}{2} D_{\text{KL}}(\pi^{\text{new}} \parallel \pi^{\text{old}})} \right].$$

Taking the expectation over $g \sim p_{\text{old}}$, applying Jensen’s inequality $\mathbb{E}[\sqrt{X}] \leq \sqrt{\mathbb{E}[X]}$, and using the definition $D_{\text{old}} \triangleq \sqrt{2\mathbb{E}_{s \sim d_{\text{old}}^{\pi^{\text{old}}}}[D_{\text{KL}}]}$:

$$|J_{\text{old}}(\pi^{\text{new}}) - J_{\text{old}}(\pi^{\text{old}})| \leq \frac{2\gamma}{(1-\gamma)^2} \underbrace{\mathbb{E}_{g \sim p_{\text{old}}}[M_g(\pi^{\text{new}})]}_{M_{\text{old}}} \cdot D_{\text{old}}.$$

A.2.2. PROOF OF PLASTICITY BOUND

For new tasks, we consider the performance gain: $J_{\text{new}}(\pi^{\text{new}}) - J_{\text{new}}(\pi^{\text{old}})$. Using Lemma A.1 with π^{old} as the anchor, for a goal $g \sim p_{\text{new}}$:

$$J_g(\pi^{\text{new}}) - J_g(\pi^{\text{old}}) = \frac{1}{1-\gamma} \mathbb{E}_{s \sim d_g^{\pi^{\text{new}}}} \left[\mathbb{E}_{a \sim \pi^{\text{new}}} [A_g^{\pi^{\text{old}}}(s, a)] \right].$$

Since $\mathbb{E}_{a \sim \pi^{\text{old}}} [A_g^{\pi^{\text{old}}}(s, a)] = 0$, we can rewrite the inner expectation:

$$\mathbb{E}_{a \sim \pi^{\text{new}}} [A_g^{\pi^{\text{old}}}] = \sum_a (\pi^{\text{new}}(a|s) - \pi^{\text{old}}(a|s)) A_g^{\pi^{\text{old}}}(s, a).$$

By Hölder’s inequality:

$$|\mathbb{E}_{a \sim \pi^{\text{new}}} [A_g^{\pi^{\text{old}}}]| \leq 2D_{\text{TV}}(\pi^{\text{new}} \parallel \pi^{\text{old}}) \cdot \sup_a |A_g^{\pi^{\text{old}}}(s, a)|.$$

For states s visited by π^{new} , the advantage is bounded by $M_g(\pi^{\text{new}})$. Applying Pinsker’s inequality:

$$\mathbb{E}_{a \sim \pi^{\text{new}}} [A_g^{\pi^{\text{old}}}] \leq M_g(\pi^{\text{new}}) \sqrt{2D_{\text{KL}}(\pi^{\text{new}} \parallel \pi^{\text{old}})}.$$

Substituting back into the PDL:

$$J_g(\pi^{\text{new}}) - J_g(\pi^{\text{old}}) \leq \frac{1}{1-\gamma} M_g(\pi^{\text{new}}) \mathbb{E}_{s \sim d_g^{\pi^{\text{new}}}} \left[\sqrt{2D_{\text{KL}}(\pi^{\text{new}} \parallel \pi^{\text{old}})} \right].$$

Taking the expectation over $g \sim p_{\text{new}}$, applying Jensen’s inequality, and using the definitions of M_{new} and D_{new} :

$$J_{\text{new}}(\pi^{\text{new}}) - J_{\text{new}}(\pi^{\text{old}}) \leq \frac{1}{1-\gamma} M_{\text{new}} \cdot D_{\text{new}}.$$

□

A.3. Corollaries and Proofs

A.3.1. BOUNDS ON ADVANTAGE MAGNITUDE

The metric $M_g(\pi^{\text{new}})$ defined in Definition A.2 depends on the magnitude of the estimated advantage \hat{A} . We show that this magnitude is naturally bounded by the critic’s approximation error (for old tasks) or the return range (for new tasks).

Corollary A.1 (Stability Control via Critic Error). *For old goals $g \in p_{\text{old}}$, assume rewards are bounded by R_{max} and the critic approximates the true value with error ε . Then $M_g(\pi^{\text{new}})$ is bounded by:*

$$M_{g_{\text{old}}}(\pi^{\text{new}}) \leq C_1 R_{\text{max}} + C_2 \varepsilon,$$

where C_1, C_2 are constants depending on γ .

Proof. (Proof omitted for brevity, follows from triangle inequality on $\hat{A} = r + \gamma V - V$ and bound analysis in Section A.3.1). □

Corollary A.2 (Plasticity Control via Return Range). *For new goals $g \in p_{\text{new}}$, if critics are fitted to MC returns bounded in $[G_{\text{min}}, G_{\text{max}}]$, let $G_{\text{abs}} = \max(|G_{\text{min}}|, |G_{\text{max}}|)$. Then:*

$$M_{g_{\text{new}}}(\pi^{\text{new}}) \leq 2(1+\gamma)G_{\text{abs}}.$$

Proof. Since \hat{A} is evaluated on trajectories collected by π^{new} (the visiting policy), the values satisfy the MC bounds. The proof follows directly from the triangle inequality $|r + \gamma V' - V| \leq |r| + \gamma|V'| + |V|$ and substituting $|V| \leq G_{\text{abs}}$. □

A.4. Corollaries and Proofs: Controlling Advantage Magnitude

In Theorem 4.1, the stability and plasticity bounds depend linearly on the advantage magnitude $M_g(\pi^{\text{new}})$. Here, we derive explicit bounds for M_g based on the critic’s approximation error (for old tasks) and the MC return range (for new tasks). These corollaries theoretically justify why minimizing critic error preserves stability and why bounding MC returns ensures safe plasticity.

A.4.1. BOUNDS FOR OLD TASKS (STABILITY)

For old tasks, the advantage $\hat{A}_{g_{\text{old}}}$ is estimated using learned value functions. We denote the true value functions of the anchored policy as V_{old} and Q_{old} .

Corollary A.3 (V-only Path Bound). *Assume the reward is bounded by $|r(s, a, g)| \leq R_{\max}$. Let the learned value function V_{θ} approximate the anchored policy’s value V_{old} with a uniform error bound $\sup_s |V_{\theta}(s, g) - V_{\text{old}}(s, g)| \leq \varepsilon_V$. Let $\|V_{\text{old}}\|_{\infty}$ denote the infinity norm of the true value function. Then:*

$$M_{g_{\text{old}}} \leq R_{\max} + (1 + \gamma) (\|V_{\text{old}}\|_{\infty} + \varepsilon_V).$$

Proof. Under the V-only path, the advantage is estimated as $\hat{A}(s, a) = r(s, a) + \gamma \mathbb{E}_{s'}[V_{\theta}(s')] - V_{\theta}(s)$. By the triangle inequality and Jensen’s inequality ($|\mathbb{E}[X]| \leq \mathbb{E}[|X|]$):

$$|\hat{A}(s, a)| \leq |r(s, a)| + \gamma \mathbb{E}_{s'}[|V_{\theta}(s')|] + |V_{\theta}(s)|.$$

Using the approximation assumption, for any state s , $|V_{\theta}(s)| \leq |V_{\text{old}}(s)| + \varepsilon_V \leq \|V_{\text{old}}\|_{\infty} + \varepsilon_V$. Substituting these bounds:

$$\begin{aligned} |\hat{A}(s, a)| &\leq R_{\max} + \gamma(\|V_{\text{old}}\|_{\infty} + \varepsilon_V) + (\|V_{\text{old}}\|_{\infty} + \varepsilon_V) \\ &= R_{\max} + (1 + \gamma)(\|V_{\text{old}}\|_{\infty} + \varepsilon_V). \end{aligned}$$

Since this bound holds for all (s, a) , it holds for the supremum over the support of any visiting policy π^{new} , thus proving the corollary. \square

Corollary A.4 (Q-only Path Bound). *Assume the learned Q-function Q_{ϕ} approximates the anchored Q-function Q_{old} with error $\sup_{s, a} |Q_{\phi}(s, a, g) - Q_{\text{old}}(s, a, g)| \leq \varepsilon_Q$. Let $\|Q_{\text{old}}\|_{\infty}$ be the supremum of the true Q-values. Then:*

$$M_{g_{\text{old}}} \leq 2(\|Q_{\text{old}}\|_{\infty} + \varepsilon_Q).$$

Proof. The Q-only advantage is $\hat{A}(s, a) = Q_{\phi}(s, a) - \mathbb{E}_{a' \sim \pi}[Q_{\phi}(s, a')]$. By the triangle inequality:

$$|\hat{A}(s, a)| \leq |Q_{\phi}(s, a)| + \sup_{a'} |Q_{\phi}(s, a')| \leq 2 \sup_{a'} |Q_{\phi}(s, a')|.$$

Using the error bound $|Q_{\phi}(s, a)| \leq \|Q_{\text{old}}\|_{\infty} + \varepsilon_Q$, we obtain:

$$|\hat{A}(s, a)| \leq 2(\|Q_{\text{old}}\|_{\infty} + \varepsilon_Q).$$

This completes the proof. \square

A.4.2. BOUNDS FOR NEW TASKS (PLASTICITY)

For new tasks, where no pre-trained critic exists, the advantage is estimated using MC returns G_t .

Corollary A.5 (MC Estimation Controls Plasticity). *Assume the value functions are fitted to MC returns bounded within $[G_{\min}, G_{\max}]$. Let $G_{\text{abs}} \triangleq \max(|G_{\min}|, |G_{\max}|)$. Then the advantage magnitude $M_{g_{\text{new}}}$ is bounded by:*

1. **V-only path:** $M_{g_{\text{new}}} \leq 2(1 + \gamma)G_{\text{abs}}$.

2. **Q-only path:** $M_{g_{\text{new}}} \leq 2G_{\text{abs}}$.

Proof. Since the critics are trained on bounded returns, we have $|V(s)| \leq G_{\text{abs}}$ and $|Q(s, a)| \leq G_{\text{abs}}$ for all states visited.

1. V-only path: Recall that the realized return satisfies $G_t = r_t + \gamma G_{t+1}$. Rearranging for reward implies $r_t = G_t - \gamma G_{t+1}$, thus $|r_t| \leq |G_t| + \gamma |G_{t+1}| \leq (1 + \gamma)G_{\text{abs}}$. Substituting this reward bound and the value bound into the advantage definition:

$$\begin{aligned} |\hat{A}(s, a)| &\leq |r| + \gamma |V(s')| + |V(s)| \\ &\leq (1 + \gamma)G_{\text{abs}} + \gamma G_{\text{abs}} + G_{\text{abs}} \\ &= 2(1 + \gamma)G_{\text{abs}}. \end{aligned}$$

2. Q-only path: Directly applying the triangle inequality to $\hat{A}(s, a) = Q(s, a) - \mathbb{E}[Q(s, \cdot)]$:

$$|\hat{A}(s, a)| \leq |Q(s, a)| + \sup_{a'} |Q(s, a')| \leq G_{\text{abs}} + G_{\text{abs}} = 2G_{\text{abs}}.$$

□

A.4.3. SUMMARY OF THEORETICAL IMPLICATIONS

These corollaries provide the mechanism for the Unified Stability–Plasticity bounds in Theorem 4.1:

- **Stability:** Corollaries A.3 and A.4 imply that stability on old tasks is governed by the quality of value function approximation $(\varepsilon_V, \varepsilon_Q)$. A well-optimized critic minimizes M_{old} , thereby tightening the trust region and preventing catastrophic forgetting.
- **Plasticity:** Corollary A.5 ensures that even during the exploration of new tasks (where π^{new} may diverge significantly from π^{old}), the advantage magnitude remains strictly bounded by the return range. This prevents destabilizing updates solely due to estimation variance, facilitating safe adaptation.

A.5. Objectives and Total Training Loss

Policy Divergence Constraint for D_{new} and D_{old} The trust region in Eq. 14 bounds D_{new} . To constrain D_{old} per Theorem 4.1, we add goal-conditioned behavior cloning on \mathcal{B}_{old} :

$$\mathcal{L}_{\text{KL}}(\theta) = \mathbb{E}_{(s, a, g) \sim \mathcal{B}_{\text{old}}} [\|\pi_\theta(\cdot | s, g) - a\|^2]. \quad (10)$$

Total Training Loss: Lagrangian Relaxation Recall our constrained continual learning objective:

$$\begin{aligned} \max_{\pi^k} \quad & J_{g_k}(\pi^k; \mathcal{T}_k) \\ \text{s.t.} \quad & J_{g_{k-1}}(\pi^k; \mathcal{T}_{k-1}) \geq J_{g_{k-1}}(\pi^{k-1}; \mathcal{T}_{k-1}) - \delta. \end{aligned} \quad (11)$$

We convert this into an unconstrained optimization via Lagrangian relaxation. By Theorem 4.1, the constraint can be decomposed into bounds on policy divergence ($D_{\text{old}}, D_{\text{new}}$) and value accuracy ($M_{\text{old}}, M_{\text{new}}$). This yields the Lagrangian:

$$\begin{aligned} \mathcal{L}(\pi, \alpha, \beta_V, \eta) = & \underbrace{-J_{g_k}(\pi^k)}_{\text{maximize new return}} \\ & + \alpha \cdot \underbrace{D_{\text{old}}(\pi^k, \pi^{k-1})}_{\text{policy divergence penalty}} \\ & + \beta_V \cdot \underbrace{M_{\text{old}}}_{\text{old value error penalty}} \\ & + \eta \cdot \underbrace{M_{\text{new}}}_{\text{new value error penalty}}, \end{aligned} \quad (12)$$

where $\alpha, \beta_V, \eta \geq 0$ are Lagrange multipliers enforcing the constraint.

We instantiate this Lagrangian with practical loss terms:

$$\mathcal{L}_{\text{total}} = \mathcal{L}_{\text{PPO}} + \alpha \mathcal{L}_{\text{KL}} + \beta_V \mathcal{L}_{\text{GCV}}^V + \eta \mathcal{L}_{\text{MC}}^V, \quad (13)$$

where:

- $\mathcal{L}_{\text{PPO}} \approx -J_{g_k}(\pi^k)$: PPO objective maximizing new-task return with D_{new} trust region;
- $\mathcal{L}_{\text{KL}} \propto D_{\text{old}}$: behavior cloning loss bounding old-task policy divergence;
- $\mathcal{L}_{\text{GCV}}^V \propto M_{\text{old}}$: frozen critic loss constraining old-task value drift;
- $\mathcal{L}_{\text{MC}}^V \propto M_{\text{new}}$: trainable critic loss ensuring new-task value accuracy.

Thus, Eq. (13) is a Lagrangian relaxation of Eq. (11), with hyperparameters α, β_V, η serving as Lagrange multipliers that balance stability (preserving old-task performance) and plasticity (learning new tasks).

B. Implementation Details

B.1. Architecture and Value Function Design

Goal-Conditioned Value Formulation The value network is conditioned on language goal g by concatenating language token embeddings with state representations (extracted from the VLA backbone) before feeding through an MLP. This design ensures sensitivity to language-conditioned goals, inheriting smoothness from the shared embedding geometry. After task transition, the value network’s sensitivity to state actions automatically adjusts through the goal-conditioned mechanism.

Dual-Critic Implementation. The policy consists of three critics on shared backbone ϕ :

- Action critic ω .
- MC critic θ_{MC} : trained on new task returns, initialized randomly for task 1
- GCV critic θ_{GCV} : copied from previous task’s MC critic at task transition, then frozen

At task $k = 1$, standard RL training optimizes $\mathcal{L}_{\text{PPO}} + \eta \mathcal{L}_{\text{MC}}^V$. Upon transition to task $k > 1$, we freeze the converged MC critic as the new GCV critic and initialize a fresh MC critic.

PPO Loss Implementation and KL Constraint Following Schulman et al. (2017), we optimize the clipped surrogate objective for each task to ensure stable policy updates. Specifically, we constrain the policy update by enforcing a KL divergence penalty between the updated policy π_θ and the reference policy π' , thereby adhering to the trust region principle. Building upon this framework, the surrogate constraint for policy divergence constrains D_{new} . The overall PPO loss is then expressed as:

$$\mathcal{L}_{\text{PPO}}(\theta) = \mathbb{E}_{(s,a,g) \sim \mathcal{B}_{\text{new}}} \left[\min \left(r_\theta(s, a, g) \hat{A}_\theta(s, a, g), \text{clip}(r_\theta(s, a, g), 1 - \epsilon, 1 + \epsilon) \hat{A}_\theta(s, a, g) \right) \right], \quad (14)$$

where ϵ is the **clipping hyperparameter** that restricts the probability ratio $r_\theta(s, a, g) = \frac{\pi_\theta(a|s,g)}{\pi_{\text{old}}(a|s,g)}$. To strictly enforce the trust region, we implement an **early stopping criterion** based on the approximate KL divergence:

$$D_{\text{KL}}(\pi' \parallel \pi_\theta) \approx \mathbb{E}_{(s,g) \sim \mathcal{B}_{\text{new}}} \left[\log \frac{\pi'(a|s,g)}{\pi_\theta(a|s,g)} \right] \leq d_{\text{targ}}, \quad (15)$$

where d_{targ} is the **target KL threshold**. The advantage \hat{A}_θ is computed using Generalized Advantage Estimation (GAE) (?):

$$\hat{A}_t = \sum_{k=0}^{\infty} (\gamma \lambda)^k \delta_{t+k}^V, \quad (16)$$

where $\gamma \in [0, 1]$ is the **discount factor**, $\lambda \in [0, 1]$ is the **GAE smoothing parameter**, and $\delta_t^V = r_t + \gamma V(s_{t+1}) - V(s_t)$ denotes the TD error.

B.2. Action-Value (Q-based) Implementation

We extend the Dual-Critic Architecture and Goal-Conditioned Value Formulation detailed in the methodology to action-value functions. This extension applies the same principles of independent dimension management to $Q(s, a, g)$, enabling precise control over stability and plasticity in the action-value space.

Goal-Conditioned Action-Value Formulation Consistent with the value function design, we leverage the shared Vision-Language Model’s embedding as the global state representation $\phi(s, g)$. To parameterize the action-value function $Q(s, a, g)$, we concatenate the continuous action vector a with the language-grounded state embedding $\phi(s, g)$ before the Multi-Layer Perceptron processing. This joint encoding ensures that Q -values inherit the metric smoothness and semantic understanding from the pretrained VLM embedding space, addressing language-goal tracking issues while incorporating action information.

Dual-Critic Architecture via Action State Value To operationalize the control of M_{old} and M_{new} within the Q-learning framework, we employ the Dual-Critic Architecture with critic decoupling: **1) Frozen GCV Q-critic θ_{GCV}** . Initialized from the old task’s converged Q-network and frozen during new task training. It serves as the anchor for stability, providing reference values $Q_{\text{old}}(s, a, g)$ to regularize backbone updates on historical data. **2) Trainable MC Q-critic θ_{MC}** . Updated on new task trajectories using MC returns. This critic remains plastic to capture the reward structure of the new task, naturally bounding M_{new} via the environment’s reward limits.

Q-based Goal-Conditioned Value Consistency (Q-GCV) The Q-based GCV mechanism enforces consistency between the current backbone’s predictions (via the frozen GCV critic) and the historical Q-values stored in the replay buffer \mathcal{B}_{old} . Unlike the value function which targets MC returns, the Q-function targets the specific state-action values Q_{old} recorded from previous interactions. The loss is formulated as the Mean Squared Error (MSE):

$$\mathcal{L}_{\text{GCV}}^Q(\phi) = \beta_Q \mathbb{E}_{(s, a, g) \sim \mathcal{B}_{\text{old}}} [\|Q_{\phi, \theta_{\text{GCV}}}(s, a, g) - Q_{\text{old}}\|^2]. \quad (17)$$

This objective constrains the shared backbone ϕ to maintain representations that, when passed through θ_{GCV} , reconstruct the historical action values, thereby minimizing performance degradation on old tasks (M_{old}).

Q-based Monte Carlo Learning To exploit the plasticity dimension (M_{new}), the Trainable MC Q critic is optimized to fit the returns $G_t^{g_{\text{new}}}$ from the current policy on the new task:

$$\mathcal{L}_{\text{MC}}^Q(\phi, \theta_{\text{MC}}) = \mathbb{E}_{(s, a, g) \sim \mathcal{B}_{\text{new}}} [\|Q_{\phi, \theta_{\text{MC}}}(s, a, g) - G_t^{g_{\text{new}}}\|^2]. \quad (18)$$

This allows the shared backbone to learn features necessary for the new task without being overly inhibited by the frozen GCV critic, as the optimization of θ_{MC} drives the embedding towards relevant new structures.

B.3. Training Procedure and Hyperparameters

All experiments are conducted based on OpenVLA-OFT (Kim et al., 2025), where the official pretrained checkpoints are adopted as the base model and LoRA adapters are applied for efficient task adaptation. Our implementation is built upon the RIPT-VLA codebase (Tan et al., 2025), and all unspecified training configurations strictly follow the settings reported in prior work. Training is performed with a LoRA rank of 32, and the detailed hyperparameter configuration is summarized in Tab. 7. Unless otherwise stated, all hyperparameters are kept consistent across experiments to ensure fair comparison. All experiments are executed on the following hardware platform: **CPU**: Intel(R) Xeon(R) Platinum 8358 @ 2.60GHz; **GPU**: NVIDIA A100-SXM4-80GB.

C. Task and Experiment Details

To systematically evaluate the robustness and scalability of our method, we construct multiple benchmarks by randomly sampling tasks from a shared task pool. Each benchmark contains a different number of object manipulation tasks, serving as controlled evaluation settings with varying task complexity and combinatorial difficulty. All benchmarks are fixed across methods and runs to ensure fair comparison.

Specifically, we evaluate our method on a subset of the **LIBERO** benchmark suite, consisting of tasks randomly sampled from the original collection to encompass various task cardinalities. We denote these benchmarks as **Task-1** through **Task-4**. Each benchmark comprises multiple task sets defined by natural language directives, primarily focusing on robotic

Table 3. More performance comparison on the multi-task learning scenario. Specific task settings in Appendix C.3. \uparrow denotes higher is better, while \downarrow denotes lower is better. The **best** and second best results are highlighted accordingly.

Method	FAR (\uparrow)	BWT (\uparrow)	FT (\uparrow)
SL (Liu et al., 2023)	<u>0.60</u>	<u>0.00</u>	<u>-0.70</u>
MTL (Liu et al., 2023)	0.54	0.17	<u>-0.70</u>
ER (Lopez-Paz & Ranzato, 2017)	0.52	-0.05	-0.65
LWF (Li & Hoiem, 2017)	0.43	<u>0.00</u>	-0.65
CRL-VLA (V)	0.63	-0.10	<u>-0.70</u>
CRL-VLA (Q)	0.33	-0.45	<u>-0.70</u>

Table 4. Comparison of continual learning metrics under different parameter settings (Only $\mathcal{L}_{\text{GCV}}^V$, Only $\mathcal{L}_{\text{GCV}}^Q$, and KL), where all experiments are conducted on the Task-4 benchmark (Appendix C.4).

PARAMETER VALUE	FAR (\uparrow)	BWT (\uparrow)	FORGETTING (\downarrow)	FT (\uparrow)
$\mathcal{L}_{\text{GCV}}^Q$				
0.00001	<u>0.97</u>	-0.02	<u>0.02</u>	-0.13
0.0001	0.94	-0.05	0.05	<u>-0.09</u>
0.001	0.93	-0.05	0.05	-0.06
0.01	0.98	0.02	0.00	-0.09
0.1	0.93	<u>0.00</u>	<u>0.02</u>	-0.06
$\mathcal{L}_{\text{GCV}}^V$				
0.00001	0.91	-0.05	0.06	-0.06
0.0001	0.91	0.00	0.00	-0.19
0.001	0.98	0.00	0.00	-0.06
0.01	<u>0.94</u>	-0.06	0.06	-0.03
0.1	0.93	<u>-0.03</u>	<u>0.02</u>	<u>-0.06</u>
KL				
0	0.91	-0.03	0.03	-0.03
0.000001	0.95	<u>-0.02</u>	0.02	-0.09
0.00001	0.98	<u>-0.02</u>	0.02	<u>-0.06</u>
0.0001	0.95	<u>-0.02</u>	0.02	-0.11
0.001	0.91	-0.05	0.05	-0.03
0.01	<u>0.96</u>	0.02	0.02	<u>-0.06</u>
0.1	0.90	<u>-0.02</u>	0.06	-0.09

pick-and-place behaviors. This setup allows us to rigorously assess the model’s instruction-following capabilities and its generalization across diverse task scales. we next detail the language instructions used for each benchmark. Each task consists of one or more natural language directives.

C.1. Task-1 Benchmark

- Task 0: “pick up the black bowl from table center and place it on the plate”
- Task 1: “pick up the black bowl next to the ramekin and place it on the plate”
- Task 2: “pick up the black bowl on the cookie box and place it on the plate”

C.2. Task-2 Benchmark

- Task 0: “pick up the orange juice and place it in the basket”, “pick up the chocolate pudding and place it in the basket”, “pick up the bbq sauce and place it in the basket”
- Task 1: “pick up the cream cheese and place it in the basket”, “pick up the milk and place it in the basket”, “pick up the tomato sauce and place it in the basket”

Table 5. Ablation study on the effects of the $\mathcal{L}_{\text{MC}}^V$ loss coefficient and the $\mathcal{L}_{\text{MC}}^Q$ loss coefficient on performance and stability. All experiments are conducted on the Task-4 benchmark (Appendix C.4).

PARAMETER COEF	FAR (\uparrow)	BWT (\uparrow)	FORGETTING (\downarrow)	FT (\uparrow)
$\mathcal{L}_{\text{MC}}^V$				
10	0.93	0.00	0.02	-0.06
1	0.95	-0.02	0.02	-0.03
0.1	0.93	-0.03	0.03	<u>-0.06</u>
0.01	0.90	-0.05	0.05	-0.13
0.001	0.85	-0.08	0.08	-0.13
$\mathcal{L}_{\text{MC}}^Q$				
10	0.98	0.05	0.00	-0.06
1	0.99	0.05	0.00	0.00
0.1	0.94	<u>0.03</u>	0.00	<u>-0.06</u>
0.01	0.85	-0.06	0.09	<u>-0.06</u>
0.001	0.92	-0.03	<u>0.08</u>	<u>-0.06</u>

Table 6. Ablation study of the Goal-Conditioned Value (GCV) network on model performance and stability. All experiments are conducted on the Task-4 benchmark (Appendix C.4). Enabling GCV leads to higher success rates (FAR) and significantly reduced forgetting.

USED GCV	FAR (\uparrow)	BWT (\uparrow)	FORGETTING (\downarrow)	FORWARD TRANSFER (\uparrow)
FALSE	0.29	-0.06	0.06	-0.72
TRUE	0.31	-0.02	0.02	-0.70

C.3. Task-3 Benchmark

- Task 0: “pick up the bbq sauce and place it in the basket”, “pick up the chocolate pudding and place it in the basket”
- Task 1: “pick up the ketchup and place it in the basket”, “pick up the salad dressing and place it in the basket”

C.4. Task-4 Benchmark

- Task 0: “put the wine bottle on the rack”, “put the cream cheese in the bowl”
- Task 1: “push the plate to the front of the stove”, “put the bowl on the stove.”
- Task 2: “put the wine bottle on top of the cabinet”, “open the top drawer and put the bowl inside.”

C.5. Baselines

1) Sequential Learning (SL) (Liu et al., 2023): This is the most straightforward continual learning method, where the VLA model is simply fine-tuned on new tasks without any specific mechanisms to prevent forgetting. 2) Multi-Task Learning (MTL) (Liu et al., 2023): This baseline algorithm learns from both new and old tasks simultaneously. 3) Learning Without Forgetting (LWF) (Li & Hoiem, 2017): This algorithm preserves existing knowledge without requiring the old data by having the new model *imitate* the old model’s predictions on new data during training (knowledge distillation). 4) Experience Replay (ER) (Lopez-Paz & Ranzato, 2017): It is a classic example of combining reinforcement learning and supervised learning, explicitly using episode memory to store samples from past tasks and converting them into gradient constraints to prevent the gradients of new tasks from degrading the performance on old tasks.

Table 7. Training hyperparameter configuration.

Parameter	Value
<i>General</i>	
LoRA Rank	32
Gradient Accumulation Steps	1
PPO Epochs	1
PPO Clip Range	0.2
PPO Clip High	0.2
Max Step Batch Size	2
Learning Rate (LoRA modules)	1.0×10^{-4}
Learning Rate (Action head)	5.0×10^{-5}
Weight Decay	1.0×10^{-4}
Gradient Clip Norm (model)	1.0
Gradient Clip Norm (header)	1.0
Total Steps M	12
Eval Interval $I_{interval}$	1
Update Times N	10
<i>CRL-VLA Weight</i>	
Q-Network Constraint (\mathcal{L}_{GCV}^Q)	0.01
Value-Head Constraint (\mathcal{L}_{GCV}^V)	0.01
KL Divergence Scale (λ_{KL})	1.0×10^{-6}
Q Loss Coef (\mathcal{L}_{MC}^Q)	1.0
Value Loss Coef (\mathcal{L}_{MC}^V)	1.0
Global Context Vector (GCV)	Enabled